Improved Recovery Time and Voltage Stability for Resistive Superconductor Fault Current Limiters

DOI : 10.36909/jer.17767

Buğra Yılmaz*, Muhsin Tunay Gençoğlu

Department of Electrical and Electronics Engineering, Faculty of Engineering, Firat University, Elazig, 23100, Turkey.

* Corresponding Author: b.yilmaz@firat.edu.tr

ABSTRACT

Fault current levels occurring in power systems force the breaking capacities of the breakers. In the power system elements, the generator, transformer, cables, etc., are exposed to the dangerous effects of fault current until the breaker clears the fault. Various limiting methods have been developed to eliminate this adverse situation in recent years. One of these methods is Superconducting Fault Current Limiters (SFCL). With the discovery of High-Temperature Superconductors (HTS), SFCL's Resistive type has become more popular. Resistive SFCL (R-SFCL), based on the non-linear resistance property of superconducting materials, limits the fault within the first half period. However, it cannot provide such a fast response after the fault. The time required to regain the superconducting state after the fault is the recovery time. For R-SFCL manufacturers, recovery time is a design parameter that must be kept short. This study examines limiting performance, recovery time, and voltage stability with the dynamic model created using MATLAB/Simulink. With the shunt breaker method proposed in the study, the recovery time was shortened, and the voltage stability improved.

Keywords: Dynamic model; Fault current limitation; MATLAB/Simulink; Recovery time; Resistive SFCL; Voltage stability.

INTRODUCTION

The increase in the world population and the development of the industry increase the electricity production day by day. The establishment of new power systems to meet the electricity demand causes the fault current levels to rise. With the breaking capacity of the breakers to be exceeded in the near future, fault-current limiting methods have become indispensable in recent years. One of the modern methods, SFCL, limits the fault current effectively and quickly by using the transition property between the superconducting and resistive regions of the superconducting material (Method, 2019) (Zampa et al., 2022). SFCL limits the fault current level and protects both breakers and other power system components (Ju et al., 2022)(Xiang, Gao, et al., 2020)(Xiang et al., 2018)(Jiahui Zhu et al., 2019). SFCL applied in power systems can be

divided into Resistive and Inductive Types. Among these two types, Resistive SFCL (R-SFCL) has advantages such as low cost, small size, simplicity, and less maintenance compared to Inductive SFCL (I-SFCL) (Noe & Steurer, 2007)(Morandi, 2013)(Xiang, Luo, et al., 2020). Another problem in power systems is that the currents encountered by the breakers increase as their breaking speed increases. This is due to the DC component of the current. R-SFCL reduces the X/R ratio, reducing the influence of the DC component and the burden on the breakers. In addition, R-SFCL can react very quickly to faults without the need for any sensors or power electronic switches, thanks to the inherent ability of the superconducting material. These mentioned advantages make R-SFCL an important point compared to I-SFCL in power system applications. In recent years R-SFCL has become more and more popular in many countries (Siyuan et al., 2019)(Pascal et al., 2017)(Yang et al., 2018)(Yadav et al., 2019) (Jiamin Zhu et al., 2022). Since the resistance of R-SFCL increases rapidly during the fault, it cannot decrease to a negligible level immediately after the fault, thus creating disadvantages such as recovery time. During this time, the nominal current is limited by the R-SFCL, causing unwelcome power loss. In some cases, it takes a few seconds for the R-SFCL to transition into the superconducting region after the fault is cleared (Noe & Steurer, 2007), while in other cases, it takes more than 300 seconds (Zhang et al., 2015).

Various methods have been tried to keep the recovery time short. Some of these studies examined the change of recovery time according to the stabilizer thickness (Sheng et al., 2016)(Kwon et al., 2010), others according to the insulation layer (Shirai et al., 2016)(Tamashima et al., 2017)(Du, 2013)(Kempski et al., 2019)(Gorbunova et al., 2020). Changing the superconductor tape architecture is one of these methods. However, this affects the entire production process, and the lamination process becomes more critical. Improvements to the cryogenic system are both costly and complex. This will significantly increase the R-SFCL investment cost and increase possible power losses from the cryogenic system. In another study, superconducting cable and R-SFCL features were combined to shorten recovery time (H. Liang et al., 2022), however, preparing the cable line for this system and installing the liquid nitrogen-filled cable structure without damage is laborious and expensive.

Apart from these solutions mentioned, the recovery time can be shortened with some changes to the R-SFCL structure. Some studies have been carried out in the literature on this subject. In the simulations for the HVDC system, the SFCL with the circuit breaker, called hybrid SFCL, offers the most desired performance in terms of interruption time, recovery time, energy dissipation, and voltage transients (H. Lee et al., 2019). Again, in the small-scale study for the DC system, the power loss on the AC side is reduced, and the DC side is safely limited (S. Liang et al., 2018). 22.9 kV/630 A hybrid SFCL implementation was installed in an AC system to shorten recovery time and increase power stability in South Korea (B. W. Lee et al., 2008)(Hyun et al., 2009)(S. Lee et al., 2010)(I. Y. Seo et al., 2013)(S. Seo et al., 2013)(C. H. Kim et al., 2014). In a later study, it was shown with simulations that the transient stability was improved with the changes made in the structure of the method (S. Seo et al., 2013). An experimental study on an AC system noted that a hybrid SFCL with a double split reactor of a different design had a shorter recovery time than a typical SFCL (Jiahui

Zhu et al., 2020). Another study examining SFCL types stated that hybrid SFCL targets factors such as reducing the required superconductor length, shortening the recovery time, and minimizing the cost (Barzegar-Bafrooei et al., 2019).

On the other hand, the voltage stability of the power system is deteriorated during the fault. The most significant factor in the formation of voltage instability in the system is the inability to meet the demanded reactive power. In the case of an increase in the reactive power demand of the loads, voltage drops occur in the busbars. With the rise in the demanded reactive power, voltage drops increase, and, in some cases, voltage collapses occur. More current is drawn from the source to compensate for these voltage drops. This situation causes the lines to consume more reactive power, leading to voltage drops and instability. To minimize these adverse situations, R-SFCL is an ideal solution and improves voltage stability (Banik & Ali, 2013). In another study examining this issue, simulations stated that hybrid SFCL improves voltage stability (Lim et al., 2011).

In this study, unlike the systems in the literature, a resistor will be used instead of a current-limiting reactor (CLR). Thus, harmonics and magnetic field interference will be eliminated, and the DC component of the fault current will be suppressed by keeping the X/R ratio low. In the literature, the driving coil, which gives the on-off signal to the breakers, manages the system at one point depending on the CLR current. In this proposed method, the control system for auxiliary and shunt breakers will be separate. Thus, the possibility of a fault in the CLR forced by high fault currents to render the system inoperable will be eliminated.

This study compares R-SFCL with shunt breaker to typical R-SFCL in terms of recovery time and voltage stability. This comparison was made by creating a dynamic model in MATLAB/Simulink. As a result of the simulations, it has been seen that R-SFCL with the shunt breaker improves recovery time and voltage stability more.

DYNAMIC MODEL

R-SFCL has been modeled based on the relationship between electric field (E) and current density (J) (Aly & Mohamed, 2012)(Chen et al., 2013)(Sousa et al., 2012)(Blair et al., 2013)(Mafra et al., 2017)(Schettino et al., 2018)(Dondapati et al., 2017). According to this model, the superconducting material can be in one of three regions: superconducting, flux-flow, and resistive. R-SFCL resistance and current density for any instant are calculated by Eq. 1 and 2, respectively (De Sousa et al., 2014)(Hatata et al., 2018)(Jiahui Zhu et al., 2015)(Nemdili & Belkhiat, 2012).

$$R_{Rsfcl}(t) = \frac{E(J,T)\ L_s}{J(t)\ A_s} \tag{1}$$

$$J(t) = \frac{I_{Rsfcl}(t)}{A_s} \tag{2}$$

where, R_{Rsfcl} is the instant R-SFCL resistance (Ω), L_s is the superconductor length (m), A_s is the superconductor section (m^2), E is the electric field as a function of J and T (V/m), T is the instant R-SFCL temperature (°K), I_{Rsfcl} is the instant R-SFCL current (A), and J is the instant current density (A/m^2).

Superconducting Region

The R-SFCL resistance is theoretically zero in this region, transmitting power without loss. E is calculated by Eq. 3 and used in Eq. 1 to calculate the instantaneous R-SFCL resistance. The conditions for this region are $E<E_0$ and $T<T_c$.

$$E(J,T) = E_c \left(\frac{J}{J_C(T)}\right)^{\alpha} \tag{3}$$

$$J_c(T) = J_c \left(\frac{T_c - T}{T_c - T_0}\right) \tag{4}$$

$$\alpha_x = \frac{\log\left({E_0}/{E_c}\right)}{log\left(\left({J_c}/{J_{c(T)}}\right)^{\left(1-\frac{1}{\beta}\right)} \left({E_0}/{E_c}\right)^{\frac{1}{\alpha}}\right)} \tag{5}$$

$$\alpha = \max[\beta, \alpha_x] \tag{6}$$

where, E_c is the critical electric field (1 μV/cm), J_c (T) is the critical current density (A/m^2) as a function of T, J_c is the critical current density at 77 °K, T_c is the critical temperature (°K), T_0 is the first temperature value (77 °K), α_x is the time-varying value of the exponential value, α is the superconducting region exponent value, the α value ranges from 5-15 for 1G HTS materials and 15-40 for 2G HTS materials (Xue et al., 2015)(Dutta & Babu, 2014)(Qian et al., 2017).

Flux-Flow Region

In this region, the temperature rises, and the rising temperature lowers J_c(T), so the electric field increases continuously. The conditions for this region are $E>E_0$ and $T<T_c$.

$$E(J,T) = E_0 . \left({E_C}/{E_0}\right)^{\beta/\alpha} \frac{J_C}{J_{C(T)}} \left({J}/{J_C}\right)^{\beta} \tag{7}$$

where, E_0 is the electric field during the transition from the superconducting region to the flux-flow region (V/m) and takes a value between 0.1 and 1 V/m, β is the exponent of the flux-flow region, for both 1G and 2G HTS materials range from 2-4 (Xue et al., 2015)(Dutta & Babu, 2014)(Qian et al., 2017).

Resistive Region

In this region, the R-SFCL temperature exceeds the critical value, its resistance increases, and the fault current is limited. The condition for this region is $T>T_c$.

$$E(J,T) = \rho(T_c)\, J\, \frac{T}{T_c} \tag{8}$$

where, $\rho(T_c)$ is the superconductor resistivity in the resistive region (Ω.m).

During the limiting process, the superconducting material heats up. After the recovery time, the cryogenic system cools the superconducting material and returns to the R-SFCL superconducting region.

The heat transfers between liquid nitrogen (LN_2) and superconducting material and R-SFCL temperature variation have been calculated with the equations given below (Jiahui Zhu et al.,

2015)(Nemdili & Belkhiat, 2012)(Manohar & Ahmed, 2012)(Elmitwally, 2009)(Langston et al., 2005) (Song et al., 2021) (H. Liang et al., 2022).

$$Q_{Rsfcl}(t) = \int I_{Rsfcl}(t)^2 \; R_{Rsfcl}(t)\, dt \tag{9}$$

$$Q_{cryosys}(t) = \int \left(\frac{T(t)-T_0}{\theta_s}\right) dt \tag{10}$$

$$\theta_s = \frac{1}{k\; L_s\; \pi\; d_s} \tag{11}$$

$$T_{Rsfcl} = T_{Rsfcl} + (Q_{Rsfcl} - Q_{cyrosys})/c_s \tag{12}$$

$$c_s = L_s\, A_s\, c_{vol} \tag{13}$$

where, Q_{Rsfcl} is the heat energy emitted by the R-SFCL (J), $Q_{cryosys}$ is the heat energy received by the cryogenic system (J), θ_s is the thermal resistance between R-SFCL and cryogenic system (K/W), k is the heat transfer coefficient to the cryogenic system (W/Km^2), d_s is the superconductor diameter (m), c_s is the superconductor heat capacity (J/K), c_{vol} is the superconductor volumetric specific heat (J/Km^3), T_{Rsfcl} is the R-SFCL instant temperature (°K). This study takes the k coefficient as a constant to simplify the model while performing thermal calculations (Jiahui Zhu et al., 2015)(Nemdili & Belkhiat, 2012)(Manohar & Ahmed, 2012)(Elmitwally, 2009)(Langston et al., 2005)(Song et al., 2021).

Today, superconducting materials are generally produced as tape. For this, instead of superconductor diameter, superconductor width and thickness parameters have been considered in the thermal resistance equation. Eq. 11 is arranged as Eq. 14 (Langston et al., 2005).

$$\theta_s = \frac{1}{2\; k\; L_s\; t_s\, w_s} \tag{14}$$

where, w_s is the superconductor tape width, and t_s is the superconductor tape thickness.

All the equations have been modeled as M-functions in MATLAB/Simulink.

The model of the power system using R-SFCL with the shunt breaker is shown in Figure 1. R-SFCL is also used with a shunt resistor. This shunt resistor can protect the superconducting material from Hot-Spot formations during the fault and prevents overvoltages if the transition to the resistive region occurs too quickly. In some studies, this shunt resistor was ignored to simplify the model (Blair et al., 2012), but in this study, its effect has been considered as recovery time has been examined. Finally, the power system and R-SFCL model parameters are as in Table 1.

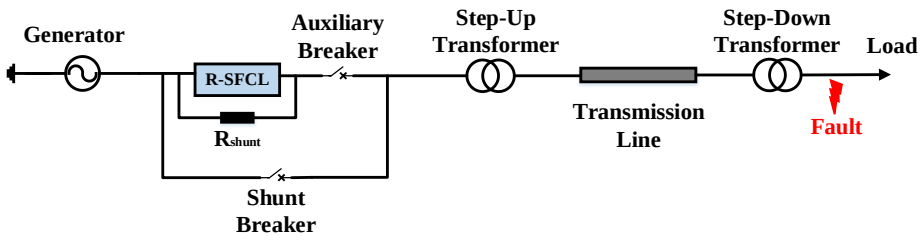

Figure 1. Power system

In the simulations, the single-phase to ground fault, which is the most likely to occur in power systems, was performed. The fault started at the 100^{th} millisecond and lasted for 100 milliseconds. The transmission line length is 25 km, and both transformers' primary and secondary resistance and inductance values are 0.002 and 0.08 in pu, respectively. Transformer powers are also 250 MVA, and simulation step time is 10^{-5} s.

Various types of superconducting materials are used in R-SFCL applications. First-generation High-Temperature Superconductors (1G HTS) or second-generation High-Temperature Superconductors (2G HTS) can be used in R-SFCL applications. 2G HTS materials have a higher current capacity, critical current level, magnetic flux value, and mechanical strength. In addition, 2G materials pass into the resistive region faster than 1G materials (S. Y. Kim & Kim, 2011). Likewise, after the fault is complete, the 1G HTS returns to the superconducting region later than the 2G HTS (Jiamin Zhu et al., 2022) and 1G HTS has a lower normal operation resistance than 2G HTS (Kulkarni et al., 2012). Therefore, in recent years, 1G HTS materials are generally used in cable applications, 2G HTS materials are used in SFCL applications. It has been accepted that 2G HTS material, which is the most common in the market today, is used as the superconducting material, and the parameters are selected accordingly.

Design Steps

The shunt breaker and the auxiliary breaker, which are used to shorten the recovery time, work in coordination. First, the system current and the R-SFCL temperature are instantaneously controlled. The current transformers will measure the system current, while sensors will be used for the R-SFCL temperature. However, this process has been done with measurement and comparison blocks to simplify the simulation. When the desired conditions are met, the breaker positions are controlled with the signal sent to the external control port on the breaker blocks in MATLAB/Simulink. Then, the breakers are opened and closed according to the duty period given in Figure 2 and the maneuver algorithm given in Figure 3. In real applications, these processes are provided by relay-breaker coordination. Before the fault, the shunt breaker is open; the auxiliary breaker is closed. The same positions apply throughout the fault. If the R-SFCL remains active after the fault is complete, it will cause power loss as the temperature has not yet dropped below the critical temperature. At this point, the advantage of R-SFCL over conventional and inefficient limiting methods is lost. For this, the shunt breaker must transmit the nominal current after the fault is complete until the temperature drops below the critical temperature and approaches 77 °K. Otherwise, the unnecessary and unwelcome nominal current limitation will continue.

Table 1. R-SFCL and power system model parameters

Parameters	Values	Parameters	Values
Source Voltage	11 kV	c_{vol}	1.5×10^6 J/K.m^3
Short Circuit Level	200 MVA	k	1.5×10^3 W/K.m^2
Frequency	50 Hz	T_0	77 °K
X/R	7	α	30
Load	10 MW, 8 MVAr	β	4

Step-Up Tr.	11/345 kV	$\rho(T_c)$	1 x 10^{-8} Ω.m
Step-Down Tr.	345/36 kV	E_c	1 μV/cm
Transmission Line	1.3225 Ω, 35.08 mH	E_0	0.1 V/m
I_c (77 °K) J_c (77 °K)	1200 A_{rms} 5 x 10^8 A_{rms}/m^2	w_s	12 mm
T_c	92 °K	t_s	0.2 mm
R_{Shunt}	3 Ω	Superconductor Tape Length	300 m

As a result, the shunt breaker is activated and deactivated according to the system current and R-SFCL temperature values, which are instantaneously controlled. The shunt breaker will not close since the system current will be more than the critical current. Thus, the shunt breaker will not disadvantage repetitive or continuous fault conditions. At the same time, the positions of these two breakers will be protected by locking mechanisms like the examples in power systems. In other words, when one is in the open position, the other will be in the closed position during all operations. It would not be mechanically possible for the opposite to occur. However, during the operation of the R-SFCL with shunt breaker, some malfunctions may be experienced as in all other methods. One of these cases is that the auxiliary breaker remains closed after the limiting operation is performed. Since the shunt breaker will be closed, the nominal current will prefer the shunt breaker instead of the high resistance R-SFCL. Thus, power loss and voltage drop will not occur in normal operating conditions. Another case is that after a fault, the auxiliary breaker remains closed, and the shunt breaker remains open before the current and temperature conditions are met. In this case, the system will behave like a typical R-SFCL and limit the nominal current with power loss and voltage drop. The last case is when the shunt breaker is closed, and the auxiliary breaker is open during the fault. In this case, the protection relay will open the shunt breaker as soon as possible and completely cut off the fault current. However, nowadays these problems are very rare with the improvements in breaker-relay coordination.

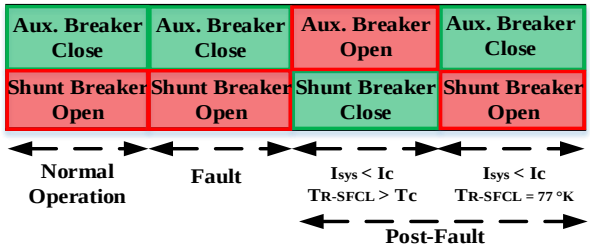

Figure 2. Breaker duty periods

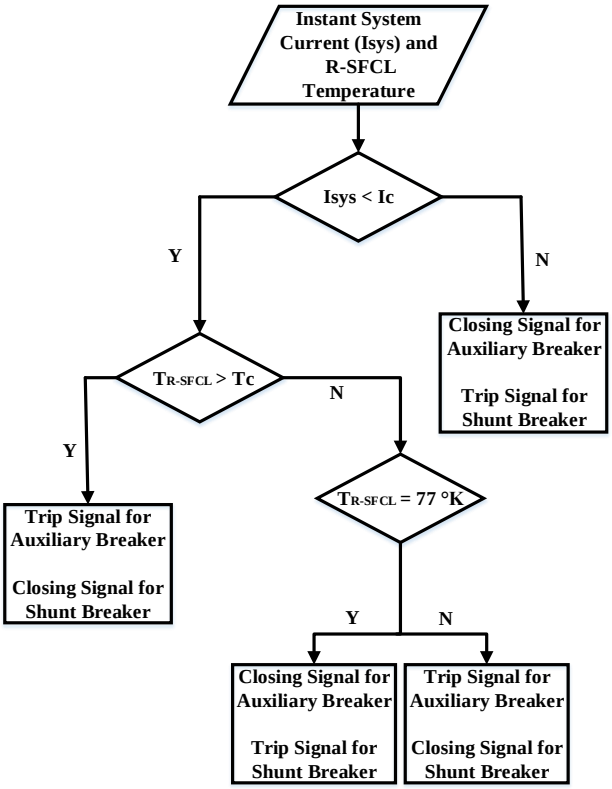

Figure 3. Breaker maneuver control algorithm

This structure, which will be installed right after the generator and includes both the breaker and the R-SFCL, will be exposed to the fault current for a long time because of the selective protection. Auxiliary breaker may trip even before Hot-Spot occurs and reaches the maximum temperature that the superconducting material can withstand during fault. In addition, the protection relays can open the auxiliary breaker after a certain period in the selective protection plan. In this case, the fault current will be cleared in the system. However, these criteria can also be taken into account in future studies. In this study, only the improvement of the recovery time was examined after the fault and proposed method; the structure other than the shunt breaker can be accepted as a combination of protection and limitation elements. R-SFCL with shunt breaker has proven feasible and reliable with its advantage (Melhem, 2012).

SIMULATION RESULTS

In this section, the limiting analysis of the dynamic model and the R-SFCL are examined first. As a result of the fault, the R-SFCL showed an effective limiting performance and reacted within the first half-period and continued to limit the current until the fault was completed. Figure 4 shows fault currents with and without R-SFCL in the power system.

As shown in Figure 4, a high-level current affects the power system elements continuously until the fault is gone in the system without R-SFCL. The first peak value can cause irreversible damage. The blue line shows the variation in fault current with the addition of a single-phase R-SFCL model to the power system. The resistance and temperature variations of the R-SFCL during the fault are shown in Figure 5.

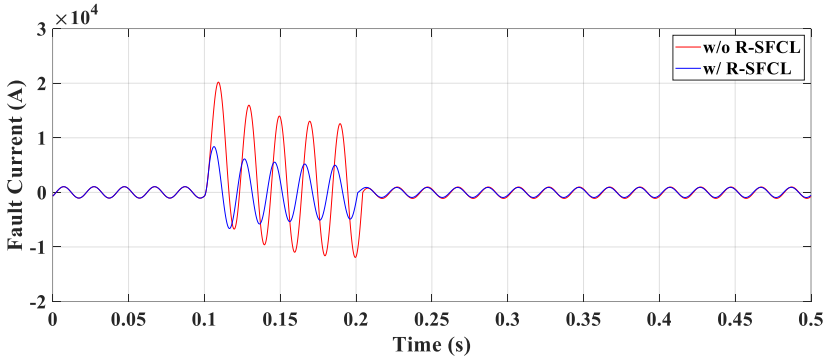

Figure 4. Fault currents

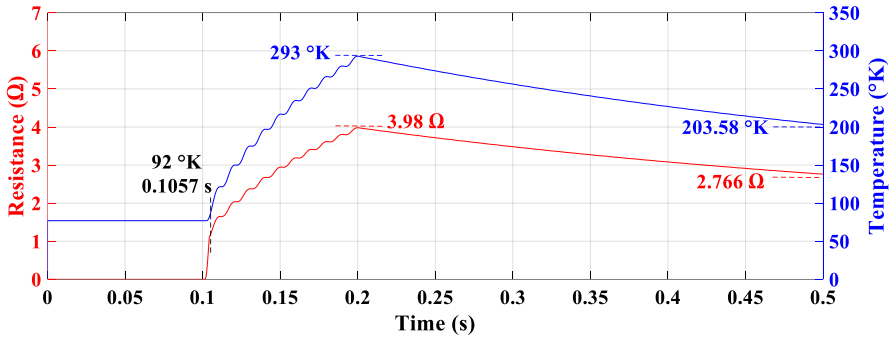

Figure 5. R-SFCL resistance and temperature

The limiting ratio and the first, second, and third peak values of the fault current are given in Table 2, respectively.

Table 2. Limiting ratio and peak values

	First Peak (kA)	Second Peak (kA)	Third Peak (kA)
w/o R-SFCL	20.2	15.96	13.96
w/ R-SFCL	8.383	6.123	5.535
Limiting Ratio (%)	58.5	61.64	60.35

It is an essential goal for manufacturers that the R-SFCL effectively reduces the first peak value of the fault current. Thus, the fault current's electromagnetic, thermal, and electrodynamic effects will be significantly reduced. As a result, larger power system elements will not be needed to provide isolation, and the economic gain will be achieved by reducing system costs.

As seen in Figure 5, 5.7 milliseconds after the fault occurred, the R-SFCL resistance suddenly increased. For a 50 Hz power system, this means reacting within the first period (de Souza et al., 2021). However, it should be noted that the R-SFCL resistance and temperature continue at a high value after the fault. Before demonstrating the advantage of the method proposed in this paper, it is necessary to focus on the post-fault situation. The system current is also shown in Figure 6 on the post-fault situation.

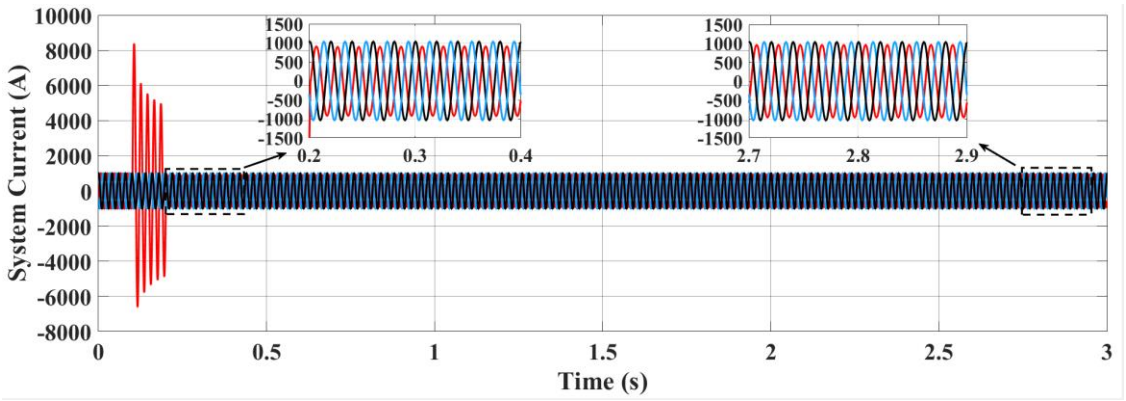

Figure 6. System current after the fault

Since the R-SFCL temperature does not drop below the critical temperature after the fault is cleared, its resistance limits the nominal current. As seen in Figure 6, while the peak value of the other phase currents is 1042.5 A after the fault, this value is 910.8 A in the faulted phase. Recovery time lasted approximately 140 seconds, and the limitation continued, albeit at a reduced rate. 3-second graphs clearly show the difference between R-SFCL with and without shunt breaker.

This decrease is due to both the R-SFCL resistance and the shunt resistor, and the power loss will continue during the recovery time. Lowering the shunt resistor value will reduce the recovery time but will negatively affect the limiting performance as it means a deliberate reduction of the equivalent resistance value. Therefore, a balanced selection must be made regarding recovery time and limiting performance. Because of lower shunt resistance, longer superconducting material is required to maintain existing limiting performance. This leads to an increase in the investment cost.

The proposed method will make the selection of shunt resistor and superconductor length less critical. Because until the R-SFCL becomes superconducting, the nominal current will flow neither through the superconducting material nor through the shunt resistor; the current will flow through the shunt breaker. This method shortens the recovery time while the limiting performance is unaffected. At the same time, the nominal current is transmitted without loss. In this case, the system current is shown in Figure 7.

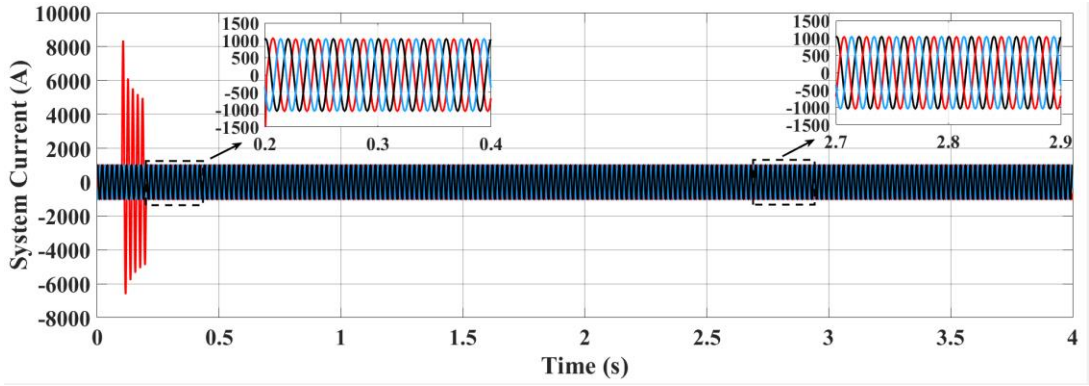

Figure 7. System current with shunt breaker

The shunt breaker removed the unwelcome limitation in the nominal current after the end of the fault. This time, because the nominal current passes through the shunt breaker, the nominal current of the phase with the fault is 1042.5 A_{peak}, just like the other phases.

The reason for this difference is the resistance and temperature variation of the R-SFCL. Figure 8 shows the resistance and temperature variation for the case with and without the shunt breaker. The dashed lines show the change without the shunt breaker, while the solid lines show the change with the shunt breaker.

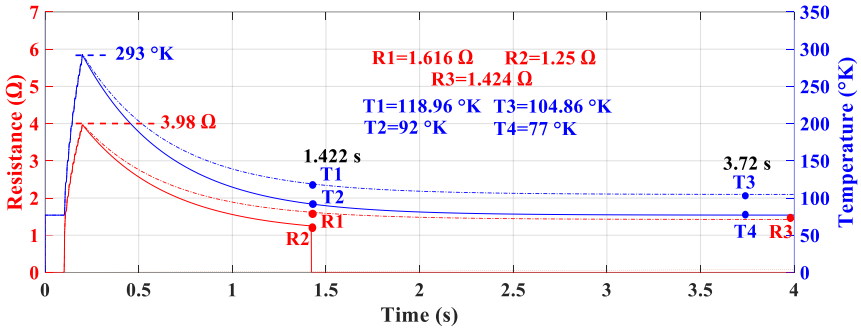

Figure 8. R-SFCL resistance and temperature variations

In the maneuver control algorithm of the breakers, the shunt breaker is set to open and the auxiliary breaker to close when the R-SFCL temperature is approximately 77 °K. This is because immediately after the R-SFCL temperature drops below 92 °K, there is a risk that it will again rise above the critical temperature relative to the level of the nominal current. In this case, the nominal current is similarly limited. This leads to instabilities in resistance and temperature graphs. Therefore, the breaker maneuvers were performed when the R-SFCL temperature was 77 °K. Approximately 3.52 s after the fault was completed, R-SFCL took the nominal current back on with the opening of the shunt breaker and transmitted the current again without loss.

The simulation results show that the shunt resistor can only prevent the Hot-Spot event and no longer affect the limiting performance. With this recommended method, recovery time, which would take 140 seconds with ordinary R-SFCL, takes 3.52 seconds. In normal operating conditions, the shunt breaker has eliminated the power loss and voltage drop.

Firstly, to examine the voltage stability, the voltage variation of the busbar at the generator output and the reactive power variation of the generator in the absence of R-SFCL are shown in Figures 9 and 10.

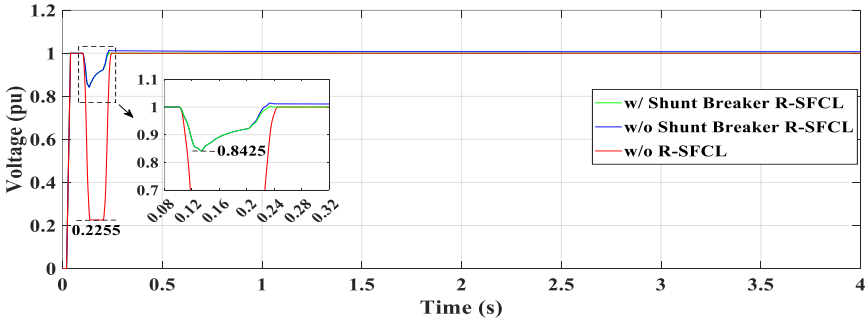

Figure 9. Voltage stability comparison

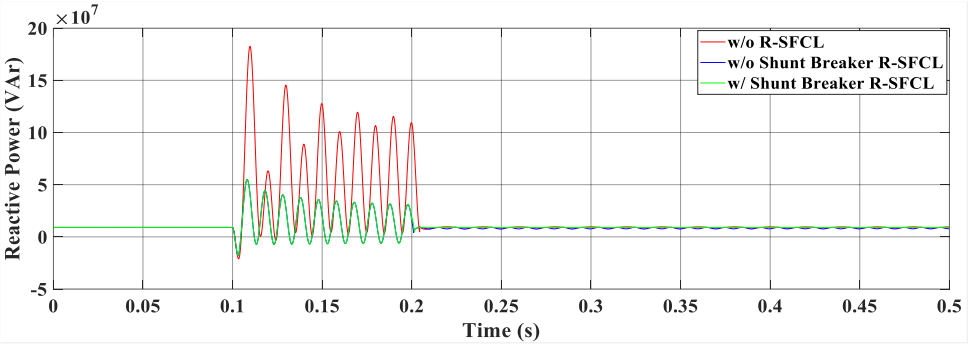

Figure 10. Reactive power comparison

As shown in Figure 9, the voltage drops to 0.2255 pu after the fault occurs without R-SFCL. With the addition of a typical R-SFCL to the system, this value was 0.8425 pu. Likewise, when there was an R-SFCL with the shunt breaker in the system, the voltage dropped to 0.8425 pu. The voltage dropped by 77.45% without R-SFCL in the system, but only 15.75% with R-SFCL. Both voltage values show that voltage stability is greatly improved with R-SFCL. On the other hand, more voltage needs to be generated by the source during the recovery period for the typical R-SFCL after the fault is complete. The blue line illustrates this situation in Figure 9. This voltage, which was over 1 pu, continued for about 140 seconds of recovery time. However, in the case of using R-SFCL with shunt breaker, the voltage quickly reached 1 pu level after the fault and did not cause an unnecessary voltage drop. The voltage drop is minimized by decreasing the reactive power value demanded with R-SFCL. Since R-SFCL with shunt breaker does not need recovery time, the reactive power immediately returned to its pre-fault state and did not cause fluctuations in the reactive power graph where it did not draw current from the source. The green line in Figure 10 shows this situation.

As seen in all simulation results, it is clear that R-SFCL with the shunt breaker shortens recovery time and improves voltage stability. All methods in the literature aiming at the same goal have both advantages and disadvantages. The table below compares the studies in the literature with the method proposed in this study.

Table 3. Comparison of methods

	Shunt Element	**Fuse Requirement**	**Driving Coil Control**	**External Limting Reactor**
The Proposed Method	Resistor	Not necessary	Separately	Not necessary
(S. R. Lee et al., 2017)	Reactor	Not necessary	At one point	Necessary
(Barzegar-Bafrooei et al., 2019)	Resistor/Reactor	Not necessary	At one point	Not necessary
(S. Seo et al., 2013)	Resistor/Reactor	Not necessary	Separately	Not necessary
(Hyun et al., 2009)	Reactor	Not necessary	At one point	Not necessary
(B. W. Lee et al., 2008)	Resistor	Necessary	At one point	Not necessary
(Romphochai & Hongesombut, 2017)	Reactor	Not necessary	At one point	Not necessary
(C. H. Kim et al., 2014)	Reactor	Not necessary	At one point	Not necessary
(S. Lee et al., 2010)	Resistor	Not necessary	At one point	Not necessary
(Lim et al., 2011)	Resistor	Not necessary	At one point	Not necessary

The method proposed in this study stands out because it does not contain a reactor and does not cause both harmonics and magnetic field interference. At the same time, it limits the fault current

faster as it reduces the X/R ratio. Another advantage is that it does not use a fuse that will need constant maintenance and an external reactor that will cause power loss in normal operation. The fact that the driving coils are separate also increases the reliability of this method. Today, the cost of superconducting materials and the need for at least two breakers for hybrid structures are the most significant barriers to the widespread use of these methods.

CONCLUSION

R-SFCL has become popular in recent years due to its advantages: small size, relatively low cost, no harmonics, no electromagnetic field interference, and increasing the X/R ratio. The use of R-SFCL increases steady-state stability and improves the power system's safety, reliability, and transient stability during fault. R-SFCL has advantages as well as disadvantages. Recovery time, which is one of these disadvantages, is a parameter that should be kept short in R-SFCL design. Otherwise, R-SFCL will not be efficient enough. There are different solutions to shorten the recovery time. Reducing the shunt resistance will reduce the limiting performance while improving the cryogenic system will increase the investment cost and maintenance.

In this study, the recovery time was shortened with a shunt breaker, and the voltage drop and power loss problems were overcome during this time. In doing so, limiting performance is preserved. Also, the superconductor tape architecture and the cryogenic system did not need to be changed. With this proposed method, the current is limited, and if necessary, it is completely eliminated with the breaker inside. In short, the breaker and R-SFCL feature are combined in a single element. As a result, this method can shorten the recovery time, which often takes minutes. This method will increase efficiency, and R-SFCL will be more quickly ready for the next fault. The proposed method, which will increase safety and reliability in power systems where fault current levels are increasing, requires two breakers and a control system in addition to the typical R-SFCL. This will increase the cost however, as seen in the simulation results, it provides energy efficiency by significantly reducing the recovery time. The energy savings provided by shortening the recovery time will tolerate the excess investment cost in the medium or long term. The shunt breaker also makes R-SFCL more reliable by minimizing the possibility of Hot-Spots. When the proposed method is installed in a switchyard in Turkey, in future studies, points such as energy efficiency, recovery time, and voltage stability will be examined with real data and the simulation will be updated accordingly. Briefly, this method is a hybrid structure in which the limiting and protection systems are gathered under a single system. Therefore, the need for the main power breaker at the generator output is eliminated thanks to this method.

REFERENCES

Aly, M. M., & Mohamed, E. A. (2012). Comparison between resistive and inductive superconducting fault current limiters for fault current limiting. *Proceedings - ICCES 2012: 2012 International Conference on Computer Engineering and Systems*, 227–232. https://doi.org/10.1109/ICCES.2012.6408518

Banik, A., & Ali, M. H. (2013). Comparison between SFCL and TSC for voltage stability enhancement of wind generator system. *2013 IEEE PES Innovative Smart Grid Technologies Conference, ISGT 2013*, 8–13. https://doi.org/10.1109/ISGT.2013.6497825

Barzegar-Bafrooei, M. R., Foroud, A. A., Ashkezari, J. D., & Niasati, M. (2019). On the advance of SFCL: A comprehensive review. *IET Generation, Transmission and Distribution*, *13*(17), 3745–3759. https://doi.org/10.1049/iet-gtd.2018.6842

Blair, S. M., Booth, C. D., & Burt, G. M. (2012). Current-time characteristics of resistive superconducting fault current limiters. *IEEE Transactions on Applied Superconductivity*, *22*(2). https://doi.org/10.1109/TASC.2012.2187291

Blair, S. M., Booth, C. D., Burt, G. M., & Bright, C. G. (2013). Application of multiple resistive superconducting fault-current limiters for fast fault detection in highly interconnected distribution systems. *IEEE Transactions on Power Delivery*, *28*(2), 1120–1127. https://doi.org/10.1109/TPWRD.2012.2228011

Chen, Y., Li, S., Sheng, J., Jin, Z., Hong, Z., & Gu, J. (2013). Experimental and numerical study of co-ordination of resistive-type superconductor fault current limiter and relay protection. *Journal of Superconductivity and Novel Magnetism*, *26*(11), 3225–3230. https://doi.org/10.1007/s10948-013-2181-9

De Sousa, W. T. B., Polasek, A., Dias, R., Matt, C. F. T., & De Andrade, R. (2014). Thermal-electrical analogy for simulations of superconducting fault current limiters. *Cryogenics*, *62*, 97–109. https://doi.org/10.1016/j.cryogenics.2014.04.015

de Souza, M. F., Queiroz, A. T., Sotelo, G. G., Monteiro, P. R. D., Fortes, M. Z., & Polasek, A. (2021). Fault current limiters: a case study of protection and operational continuity for FPSOs. *Electrical Engineering*, *103*(4), 2035–2045. https://doi.org/10.1007/s00202-021-01213-9

Dondapati, R. S., Kumar, A., Kumar, G. R., Usurumarti, P. R., & Dondapati, S. (2017). Superconducting magnetic energy storage (SMES) devices integrated with resistive type superconducting fault current limiter (SFCL) for fast recovery time. *Journal of Energy Storage*, *13*, 287–295. https://doi.org/10.1016/j.est.2017.07.005

Du, H. I. (2013). Evaluation on resistance tendency and recovery characteristics of 2G wire with insulation layer. *IEEE Transactions on Applied Superconductivity*, *23*(3), 0–3. https://doi.org/10.1109/TASC.2013.2240371

Dutta, S., & Babu, B. C. (2014). Modelling and analysis of resistive Superconducting Fault Current Limiter. *IEEE TechSym 2014 - 2014 IEEE Students' Technology Symposium*, 362–366. https://doi.org/10.1109/TechSym.2014.6808076

Elmitwally, A. (2009). Proposed hybrid superconducting fault current limiter for distribution systems. *International Journal of Electrical Power and Energy Systems*, *31*(10), 619–625. https://doi.org/10.1016/j.ijepes.2009.06.002

Gorbunova, D. A., Kumarov, D. R., Scherbakov, V. I., Sim, K., & Hwang, S. (2020). Influence of polymer coating on SFCL recovery under load. *Progress in Superconductivity and Cryogenics (PSAC)*, *12*(1), 44–47. https://doi.org/10.9714/psac.2019.21.4.044

Hatata, A. Y., Ebeid, A. S., & El-Saadawi, M. M. (2018). Application of resistive super conductor fault current limiter for protection of grid-connected DGs. *Alexandria Engineering Journal*, *57*(4), 4229–4241. https://doi.org/10.1016/j.aej.2018.11.009

Hyun, O. B., Park, K. B., Sim, J., Kim, H. R., Yim, S. W., & Oh, I. S. (2009). Introduction of a hybrid SFCL in KEPCO grid and local points at issue. *IEEE Transactions on Applied Superconductivity*, *19*(3), 1946–1949. https://doi.org/10.1109/TASC.2009.2018256

Ju, P., Ma, T., Zhang, J., Xu, Y., & Dai, S. (2022). Influence of Interface Resistance on Current Distribution and Inhomogeneity Effect on Quench Characteristics in REBCO Coated Conductor. *IEEE Transactions on Applied Superconductivity*, *32*(1). https://doi.org/10.1109/TASC.2021.3132011

Kempski, A., Rusinski, J., & Hajdasz, S. (2019). Analysis of Recovery Time of HTS Tapes with Electrical Insulation Layers for Superconducting Fault Current Limiters under Load Conditions. *IEEE Transactions on Applied Superconductivity*, *29*(8). https://doi.org/10.1109/TASC.2019.2952315

Kim, C. H., Seo, H. C., Rhee, S. B., & Kim, C. H. (2014). Decision of optimal insertion resistance of superconducting fault current limiter for reducing asymmetrical fault current. *12th IET International Conference on Developments in Power System Protection, DPSP 2014*, 1–4.

Kim, S. Y., & Kim, J. O. (2011). Reliability evaluation of distribution network with DG considering the reliability of protective devices affected by SFCL. *IEEE Transactions on Applied Superconductivity*, *21*(5), 3561–3569. https://doi.org/10.1109/TASC.2011.2163187

Kulkarni, S., Dixit, M., & Pal, K. (2012). *Study on recovery performance of high T c superconducting tapes for resistive type superconducting fault current limiter applications*. *36*, 1231–1235. https://doi.org/10.1016/j.phpro.2012.06.281

Kwon, N. Y., Kim, H. S., Kim, K. L., Hahn, S., Kim, H. R., Hyun, O. B., Kim, H. M., Kim, W. S., Park, C., & Lee, H. G. (2010). The effects of a stabilizer thickness of the YBCO coated conductor (CC) on the quench/recovery characteristics. *IEEE Transactions on Applied Superconductivity*, *20*(3), 1246–1249. https://doi.org/10.1109/TASC.2009.2039864

Langston, J., Steurer, M., Woodruff, S., Baldwin, T., & Tang, J. (2005). A generic real-time computer simulation model for superconducting fault current limiters and its application in system protection studies. *IEEE Transactions on Applied Superconductivity*, *15*(2 PART II), 2090–2093. https://doi.org/10.1109/TASC.2005.849459

Lee, B. W., Park, K. B., Sim, J., Oh, I. S., Lee, H. G., Kim, H. R., & Hyun, O. B. (2008). Design and experiments of novel hybrid type superconducting fault current limiters. *IEEE Transactions on Applied Superconductivity*, *18*(2), 624–627. https://doi.org/10.1109/TASC.2008.920785

Lee, H., Asif, M., Park, K., Mun, H., & Lee, B. (2019). *Appropriate Protection Scheme for DC Grid Based on the Half Bridge Modular Multilevel Converter System*.

Lee, S. R., Lee, J. J., Yoon, J., Kang, Y. W., & Hur, J. (2017). Protection Scheme of a 154-kV SFCL Test Transmission Line at the KEPCO Power Testing Center. *IEEE Transactions on Applied Superconductivity*, *27*(4), 2–6. https://doi.org/10.1109/TASC.2017.2669159

Lee, S., Yoon, J., & Lee, B. (2010). Analysis model development and specification proposal of hybrid Superconducting Fault Current Limiter (SFCL). *Physica C: Superconductivity and Its Applications*, *470*(20), 1615–1620. https://doi.org/10.1016/j.physc.2010.05.174

Liang, H., Chen, Y., Duan, R., Lu, Y., & Sheng, J. (2022). Numerical Study on the On-Grid Performance of Superconducting Cable Cooperated with R-SFCL. *IEEE Transactions on Applied Superconductivity*, *32*(4). https://doi.org/10.1109/TASC.2022.3141039

Liang, S., Xia, Z., & Wang, Z. (2018). Tests and Analysis of a Small-Scale Hybrid-Type. *Ieee Transactions on Applied Superconductivity*, *28*(4), 1–6.

Lim, S. H., Kim, J. S., & Kim, J. C. (2011). Analysis on protection coordination of hybrid SFCL with protective devices in a power distribution system. *IEEE Transactions on Applied Superconductivity*, *21*(3 PART 2), 2170–2173. https://doi.org/10.1109/TASC.2010.20935931

Mafra, G. R. F. Q., Sotelo, G. G., Fortes, M. Z., & de Sousa, W. T. B. (2017). Application of resistive superconducting fault current limiters in offshore oil production platforms. *Electric Power Systems Research*, *144*, 107–114. https://doi.org/10.1016/j.epsr.2016.11.006

Manohar, P., & Ahmed, W. (2012). Superconducting fault current limiter to mitigate the effect of DC line fault in VSC-HVDC system. *2012 International Conference on Power, Signals, Controls and Computation, EPSCICON 2012*, *October 2016*. https://doi.org/10.1109/EPSCICON.2012.6175282

Melhem, Z. (2012). *High temperature superconductors (HTS) for energy applications*.

Method, C. (2019). *Numerical Study on Transient State of Inductive Fault Current Limiter Based on Field-Circuit*.

Morandi, A. (2013). State of the art of superconducting fault current limiters and their application to the electric power system. *Physica C: Superconductivity and Its Applications*, *484*, 242–247. https://doi.org/10.1016/j.physc.2012.03.004

Nemdili, S., & Belkhiat, S. (2012). Modeling and simulation of resistive superconducting fault-current limiters. *Journal of Superconductivity and Novel Magnetism*, *25*(7), 2351–2356. https://doi.org/10.1007/s10948-012-1685-z

Noe, M., & Steurer, M. (2007). *High-temperature superconductor fault current limiters : concepts , applications , and development status*. https://doi.org/10.1088/0953-2048/20/3/R01

Pascal, P. T., Badel, A., Auran, G., & Pereira, G. S. (2017). Superconducting fault current limiter for ship grid simulation and demonstration. *IEEE Transactions on Applied Superconductivity*, *27*(4), 1–5. https://doi.org/10.1109/TASC.2017.2674964

Qian, K., Guo, Z., Terao, Y., & Ohsaki, H. (2017). Electromagnetic and thermal design of superconducting fault current

limiters for DC electric systems using superconducting. *20th International Conference on Electrical Machines and Systems, ICEMS 2017*.

Romphochai, S., & Hongesombut, K. (2017). *Calculation of current limiting reactance of hybrid SFCL for low voltage ride-through capability enhancement in DFIG wind farms*. 4685–4695. https://doi.org/10.3906/elk-1703-53

Schettino, H. J., Jr, R. D. A., Polasek, A., Kottonau, D., & Sousa, W. T. B. De. (2018). *A strategy for protection of high voltage systems using resistive superconducting fault current limiters Physica C : Superconductivity and its applications A strategy for protection of high voltage systems using resistive superconducting fault current lim*. *January*. https://doi.org/10.1016/j.physc.2017.11.004

Seo, I. Y., Hyun, O. B., Kim, H., Ha, B. N., Song, I. K., Chae, W., Kim, M. J., & Kim, S. J. (2013). Empirical modeling of cryogenic system for hybrid SFCL using support vector regression. *Journal of Superconductivity and Novel Magnetism*, *26*(4), 1265–1273. https://doi.org/10.1007/s10948-012-1965-7

Seo, S., Kim, S., Moon, Y., & Lee, B. (2013). A hybrid superconducting fault current limiter for enhancing transient stability in Korean power systems. *Physica C: Superconductivity and Its Applications*, *494*, 331–334. https://doi.org/10.1016/j.physc.2013.04.025

Sheng, J., Zeng, W., Ma, J., Yao, Z., Li, Z., Jin, Z., & Hong, Z. (2016). Study of recovery characteristics of 2nd generation HTS tapes with different stabilizers for resistive type superconducting fault current limiters. *Physica C: Superconductivity and Its Applications*, *521–522*, 33–37. https://doi.org/10.1016/j.physc.2016.01.002

Shirai, Y., Yoneda, K., Higa, D., Shiotsu, M., Honda, Y., & Isojima, S. (2016). Recovery Characteristics of GdBCO Superconducting Tape With Cooling Fins and Teflon Coating for Resistive Fault Current Limiter. *IEEE Transactions on Applied Superconductivity*, *26*(3), 8–11. https://doi.org/10.1109/TASC.2016.2524456

Siyuan, L., Yuejin, T., Li, R., Ying, X., Wei, W., Ziheng, H., & Bin, Z. (2019). *Physica C : Superconductivity and its applications A novel simplified modeling method based on R – Q curve of resistive type SFCL in power systems*. *563*(April), 82–87. https://doi.org/10.1016/j.physc.2019.04.016

Song, W., Pei, X., Alafnan, H., Xi, J., Zeng, X., Yazdani-Asrami, M., Xiang, B., & Liu, Z. (2021). Experimental and Simulation Study of Resistive Helical HTS Fault Current Limiters: Quench and Recovery Characteristics. *IEEE Transactions on Applied Superconductivity*, *31*(5). https://doi.org/10.1109/TASC.2021.3061958

Sousa, W. T. B. De, Polasek, A., Silva, F. A., Dias, R., Jurelo, A. R., & Andrade, R. De. (2012). Simulations and Tests of MCP-BSCCO-2212 Superconducting Fault Current Limiters. *IEEE Transactions on Applied Superconductivity*, *22*(2), 5600106. https://doi.org/10.1109/TASC.2012.2187189

Tamashima, M., Takaya, S., Shirai, Y., Shiotsu, M., Honda, G., & Isojima, S. (2017). Improvement of recovery characteristics of REBCO tape with several surface conditions for resistive fault current limiter. *IEEE Transactions on Applied Superconductivity*, *27*(4), 2–6. https://doi.org/10.1109/TASC.2017.2669150

Xiang, B., Gao, L., Luo, J., Wang, C., Nan, Z., Liu, Z., Geng, Y., Wang, J., & Yanabu, S. (2020). A CO 2 /O 2 Mixed Gas DC Circuit Breaker with Superconducting Fault Current-Limiting Technology. *IEEE Transactions on Power Delivery*, *35*(4), 1960–1967. https://doi.org/10.1109/TPWRD.2019.2957499

Xiang, B., Liu, Z., Wang, C., Nan, Z., Geng, Y., Wang, J., & Yanabu, S. (2018). DC Interrupting With Self-Excited Oscillation Based on the Superconducting Current-Limiting Technology. *IEEE Transactions on Power Delivery*, *33*(1), 529–536. https://doi.org/10.1109/TPWRD.2017.2718589

Xiang, B., Luo, J., Gao, L., Liu, Z., Geng, Y., Wang, J., & Yanabu, S. (2020). Study on the Parameter Requirements for Resistive-Type Superconducting Fault Current Limiters Combined with Mechanical DC Circuit Breakers in Hybrid AC/DC Transmission Grids. *IEEE Transactions on Power Delivery*, *35*(6), 2865–2875. https://doi.org/10.1109/TPWRD.2020.2981870

Xue, S., Gao, F., Sun, W., & Li, B. (2015). Protection principle for a DC distribution system with a resistive superconductive fault current limiter. *Energies*, *8*(6), 4839–4852. https://doi.org/10.3390/en8064839

Yadav, S., Bharati, K., & Tewari, V. (2019). *Superconducting Fault Current Limiter-A Review*. *14*(2), 1–6.

Yang, K., Yang, Y., Junaid, M., Liu, S., Liu, Z., Geng, Y., & Wang, J. (2018). Direct-Current Vacuum Circuit Breaker with Superconducting Fault-Current Limiter. *IEEE Transactions on Applied Superconductivity*, *28*(1), 1–7. https://doi.org/10.1109/TASC.2017.2767500

Zampa, A., Holleis, S., Badel, A., Tixador, P., Bernardi, J., & Eisterer, M. (2022). Influence of Local Inhomogeneities in the REBCO Layer on the Mechanism of Quench Onset in 2G HTS Tapes. *IEEE Transactions on Applied Superconductivity*, *32*(3). https://doi.org/10.1109/TASC.2022.3151950

Zhang, X., Ruiz, H. S., Zhong, Z., & Coombs, T. A. (2015). *Implementation of Resistive Type Superconducting Fault Current Limiters in Electrical Grids: Performance Analysis and Measuring of Optimal Locations*. 1–18. http://arxiv.org/abs/1508.01162

Zhu, Jiahui, Zhang, H., Chen, P., Zhao, Y., Qin, H., Wei, D., Lu, K., Dong, Y., Zhang, K., & Du, Q. (2020). Experimental investigation of current limiting characteristics for a novel hybrid superconducting fault current limiter (SFCL) with biased magnetic field. *Journal of Physics: Conference Series*, *1559*(1). https://doi.org/10.1088/1742-6596/1559/1/012104

Zhu, Jiahui, Zhao, Y., Chen, P., Jiang, S., Wang, S., Fang, J., Zhao, X., & Wang, H. (2019). Magneto-Thermal Coupling Design and Performance Investigation of a Novel Hybrid Superconducting Fault Current Limiter (SFCL) With Bias Magnetic Field Based on MATLAB / SIMULINK. *IEEE Transactions on Applied Superconductivity*, *29*(2), 1–5. https://doi.org/10.1109/TASC.2019.2892295

Zhu, Jiahui, Zheng, X., Qiu, M., Zhang, Z., Li, J., & Yuan, W. (2015). Application Simulation of a Resistive Type Superconducting Fault Current Limiter (SFCL) in a Transmission and Wind Power System. *Energy Procedia*, *75*, 716–721. https://doi.org/10.1016/j.egypro.2015.07.498

Zhu, Jiamin, Chen, S., & Jin, Z. (2022). Progress on Second-Generation High-Temperature Superconductor Tape Targeting Resistive Fault Current Limiter Application. *Electronics (Switzerland)*, *11*(3). https://doi.org/10.3390/electronics11030297